Journal of Materials Chemistry C

ROYAL SOCIETY OF CHEMISTRY

PAPER

View Article Online
View Journal | View Issue

Cite this: J. Mater. Chem. C, 2024, 12, 13884

Accurate & cheap calculations of the lowest triplet state energy: an experimentalist's guide†

Murad J. Y. Tayebjee, ‡*[a] Kin Long Kelvin Lee§[b] and Timothy W. Schmidt ‡[c]

Received 31st May 2024,
Accepted 18th July 2024

DOI: 10.1039/d4tc02241f

rsc.li/materials-c

Triplet–triplet annihilation and singlet fission are bimolecular processes which can be exploited in a range of technological applications. These processes involve the first excited singlet and triplet states (S_1 and T_1), and have restrictions on their relative energies. While singlet–singlet energy differences are easily measured using optical spectroscopy, the singlet–triplet energy gap is less amenable to experiment. We report a computationally inexpensive method for the calculation of the energy of the lowest singlet–triplet transition for a range of extended π chromophores. Excellent correlation (mean absolute displacement $\lesssim$0.05 eV) between experiment and calculation is achieved for a wide range of molecules without requiring zero point energy calculations. This provides the experimental chemist with the necessary tools to accurately predict T_1 energies for novel molecules that are candidates for triplet–triplet annihilation or singlet fission.

1. Introduction

Singlet fission (SF) and triplet–triplet annihilation (TTA) upconversion are processes with applications in efficient molecular photovoltaic devices,[1–5] 3D printing,[6] and quantum/excitonic logic devices.[7,8]

Both processes are bichromophoric and can occur in solution or solid phases; in SF an excited singlet generates two excited triplets, and the reverse occurs in TTA. As such, they are constricted to opposing energetic requirements on the energies of the first excited triplet (E_{T_1}) and singlet (E_{S_1}) states. For exothermic SF and TTA, $E_{S_1} \geq 2E_{T_1}$ and $E_{S_1} \leq 2E_{T_1}$, respectively. In both cases it is ideal for $2E_{T_1} < E_{T_2}$, to avoid TTA events giving rise to molecules in the T_2 state (where E_{T_2} is the energy of the second excited triplet state). Further, small spin–orbit coupling and the consequent low rate of intersystem crossing, is required for efficient SF and TTA so that loss mechanisms, $S_1 \rightarrow T_1$ and $T_1 \rightarrow S_0$, are unfavourable.

The energy of the first excited singlet state is easily identified by optical absorption or emission spectroscopy; the energy difference between the T_1 and T_2 state is also measured relatively easily using transient absorption techniques. However, the energy of the T_1 state is less amenable to measurement in condensed phase systems with small spin–orbit coupling. The solvent perturbation technique has been used to enhance spin–orbit coupling and measure absorption arising from the $^1\pi\pi \rightarrow {}^3\pi\pi^*$ transition.[9] However, the extinction coefficient of this transition is still extremely low (<1 cm^{-1} M^{-1}), necessitating the use of highly pure samples. Conversely, phosphorescence can be observed in similarly perturbed systems.[10] However, this often requires a triplet sensitizer and the complete removal of triplet quenchers such as O_2. Triplet energies have also been measured using engineered solid-state host matrices which allow for room-temperature phosphorescence.[11] Finally, by studying the dynamics of triplet energy transfer from a number of triplet sensitizers an estimation of the T_1 state energy can be made.[12] All of the above techniques are cumbersome in one way or another. It would be ideal to be able to estimate the T_1 energy of a candidate SF or TTA molecule using inexpensive calculations.

Much work in SF has been focused on linear polyacenes such as tetracenes[13–26] and pentacenes,[13,27–30] perylene diimides (PDI),[31–33] benzofurans,[34,35] and carotenoids.[36–40] TTA-upconversion (TTA-UC) experiments have generally used aromatic hydrocarbons as emitters, but other systems have also been studied.[41–43] It would be useful to be able to estimate the T_1 energy through calculations in order to identify whether SF or TTA is a viable process for a given molecule. However, accurate (on the order of meV) determinations of state energies of these molecules quickly becomes too expensive for any conventional post Hartree–Fock methods since the high level

[a] School of Photovoltaic and Renewable Energy Engineering, UNSW, Sydney, NSW 2052, Australia. E-mail: m.tayebjee@unsw.edu.au
[b] School of Chemistry, UNSW, Sydney, NSW 2052, Australia
[c] School of Chemistry, ARC Centre of Excellence in Exciton Science, UNSW, Sydney, NSW 2052, Australia

† Electronic supplementary information (ESI) available: Vertical transition energies are included for a subset of the basis sets studied in this work. The experimental and calculated values for test set #2 are also provided. See DOI: https://doi.org/10.1039/d4tc02241f

‡ These authors contributed equally to this work.

§ Present address: Intel Corporation 2111 25th NE Ave, Hillsboro OR 97124, USA.

wavefunction based methods such as (EOM)-CCSD and MRCI are restricted to much smaller systems. On the other hand, density functional theory (DFT) methods have proved to be an inexpensive and efficient path to ground state molecular properties. By introducing linear response methods, time-dependent DFT (TD-DFT) makes excited states of large molecules a soluble goal, which for wavefunction methods would otherwise prove intractable. TD-DFT has been used to predict excited states of molecules, with extensive systematic studies of singlet excited states,[44] triplet systems,[45] using collective excitations for crystalline arrays.[46] The resulting vertical energies depend on the functional form used, with mean absolute errors typically on the order of 0.25 eV and 0.7 eV.[47,48] We are interested in polyaromatic hydrocarbons (PAH) and other aromatic chromophores which are commonly found in systems that undergo TTA or SF. Parac and Grimme performed one of the first benchmarks on the performance of TD-DFT on PAHs.[49] In their study, the singlet–triplet energy gap was calculated for a variety of unsaturated molecules, with very promising accuracy shown for both B86 and B3LYP functionals with large basis sets. However, these calculations become time-consuming in the case of large molecules.

In this work we propose a simple method of accurately estimating the lowest singlet–triplet energy difference. Using a range of molecules with known E_{T_1}, we show that a systematic error is found by performing calculations using time independent DFT. We use a systematic overestimate to adjust the calculated triplet values in a method analogous to shifting vibrational frequencies using a scalar factor.[50] The remainder of this article is organized as follows. First we use a number of PAH molecules as a training set to establish the systematic error between experiment and calculation. Second, we test the efficacy of this method with two test sets: (i) PAH molecules and (ii) heteroatomic conjugated chromophores. Finally, we make predictions of the energy of E_{T_1} using the results of the training set and both test sets in some molecules which are pertinent to SF or TTA applications.

2. Computational details

All calculations except Section 3.4 were carried out using GAMESS-US 2013 R1.[51,52] Ground state geometries were optimized using HF,[53] or B3LYP,[54–56] or ωB97X-D[57,58] functionals and STO-3G,[59,60] 3-21G,[61,62] 6-31G,[63,64] 6-311G,[65] or 6-311+G[65,66] basis sets. Where applicable, the open shell variants were used. In the case of HF geometry optimizations, subsequent single point energy calculations were carried out with B3LYP. The triplet energy, E_{T_1}, was determined by subtracting the energy of the ground singlet state ($^1\pi\pi$) from that of the lowest triplet state ($^3\pi\pi^*$) without accounting for the zero point energy. Vertical transition energies, E_{aT_1} and E_{pT_1}, were respectively calculated by using the ground singlet and triplet state geometry for comparison with the band maxima in experimental absorption and phosphorescence spectra, as shown in the inset of Fig. S1 (ESI†).

Calculations in Section 3.4 were carried out using GAMESS-US 2023 R1.[67] Vertical triplet energies and TD-DFT calculations are carried out using the S_0 geometry optimised using B3LYP[54–56] and the aug-cc-pVTZ[68] basis set.

3. Results and discussion

3.1. PAH training set and first test set

Fig. 2 summarizes the calculations for the PAHs shown in Fig. 1. Due to the Jahn–Teller effect the symmetries of

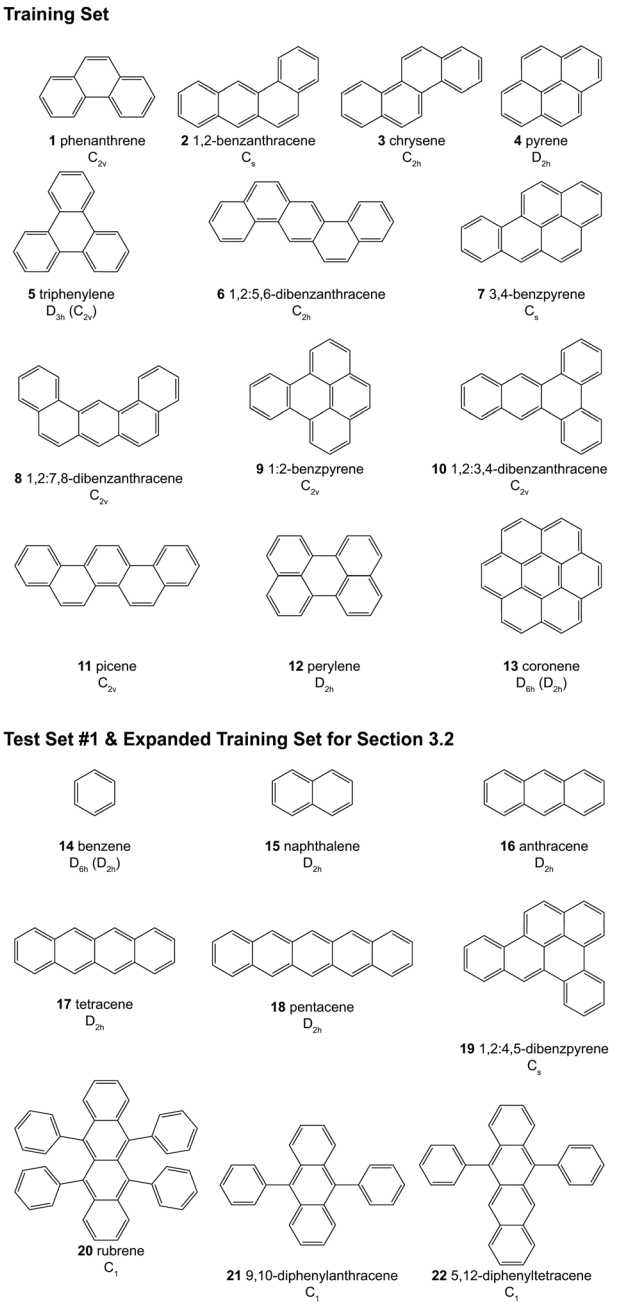

Fig. 1 The PAHs used as the training and first test set in this work. The symmetries of the calculations are also shown with triplet state symmetries shown in parentheses where they differ from the singlet state.

Table 1 Calculated first excited triplet state energies, $E_{T,calc}$, of PAHs in eV using different levels of theory

No.	Experimental conditions	$E_{T,exp}$[a]	HF/6-311G//B3LYP/6-311+G	HF/6-31G//B3LYP/6-31G	B3LYP/6-31G	B3LYP/3-21G	B3LYP/STO-3G	B3LYP/VTZ//B3LYP/cc-pVTZ[h]	HF/6-311G	HF/6-31G	ωb97x-D/3-21G
Phenanthrene **1**	Hexane 77 K	2.70	3.09	3.10	2.93	2.97	3.11	2.77	2.89	2.89	3.21
1,2-Benzanthracene **2**	EPA, 77 K	2.05	2.28	2.29	2.20	2.25	2.38	2.08	2.03	2.02	2.45
Chrysene **3**	*n*-Heptane, 77 K	2.49	2.73	2.72	2.66	2.70	2.81	2.53	2.71	2.72	2.93
Pyrene **4**	EPA, 77 K	2.08	2.25	2.25	2.25	2.28	2.37	2.16	2.49	2.49	2.47
Triphenylene **5**	EPA, 77 K	2.88	3.28	3.32	3.28	3.31	3.53	2.87	3.59	3.62	3.60
1,2:5,6-Dibenzanthracene **6**	EPA, 77 K	2.26	2.56	2.58	2.45	2.50	2.67	2.26	2.35	2.35	2.78
3,4-Benzyrene **7**	EPA, 77 K	1.82	1.95	1.94	1.90	1.94	2.00	1.83	2.01	2.00	2.12
1,2:7,8-Dibenzanthracene **8**	EPA, 77 K	2.29	2.56	2.58	2.48	2.52	2.69	2.28	2.35	2.36	2.79
1:2-Benzpyrene **9**	EPA, 77 K	2.29	2.53	2.55	2.50	2.54	2.68	2.16	2.89	2.91	2.82
1,2:3,4-Dibenzanthracene **10**	EPA, 77 K	2.20	2.42	2.45	2.36	2.41	2.58	2.22	2.17	2.18	2.64
Picene **11**	EPA, 77 K	2.49	2.80	2.79	2.72	2.75	2.88	2.51	3.25	3.25	3.08
Perylene **12**	Single crystal, 4.2 K	1.53[d]	1.64	1.67	1.66	1.70	1.88	1.54	2.07	2.09	1.97
Coronene **13**	*n*-Hexane, 77 K	2.40	2.77	2.79	2.76	2.77	2.96	2.35	3.41	3.44	3.17
Benzene **14**	Cyclohexane, 77 K	3.66	3.98	4.01	4.01	4.07	4.15	—	3.36	3.40	4.14
Naphthalene **15**	Hexane, 298 K	2.64	2.86	2.87	2.86	2.91	3.05	2.73	3.03	3.04	3.10
Anthracene **16**	EPA, 77 K	1.85	1.98	1.98	1.93	1.97	2.06	—	1.68	1.66	2.12
Tetracene **17**	Ethyl iodide, 295 K	1.27[b]	1.33	1.33	1.33	1.37	1.47	—	1.38	1.36	1.54
Pentacene **18**	Guest–host crystal	0.86[c]	0.98	0.97	0.90	0.94	1.04	—	0.69	0.67	1.09
1,2:5,6-Dibenzpyrene **19**	EPA, 77 K	2.03	2.25	2.26	2.16	2.19	2.32	—	2.33	2.33	2.46
Rubrene **20**	Benzene, RT	1.14[e]	1.35	1.34	1.12	1.18	1.25	—	0.87	0.85	1.35
9,10-Diphenylanthracene **21**	Blended polymer film	1.77[f]	1.90	1.90	1.83	1.89	1.91	—	1.57	1.57	2.02
5,12-Diphenyltetracene **22**	Benzene, RT	1.20[g]	1.39	1.38	1.29	1.33	1.39	—	1.11	1.11	1.48

[a] Value from phosphorescence experiments results in Table 6.3 of ref. 70 unless otherwise specified. [b] Value taken from absorption spectra.[9] [c] Value take the heterofission rate of pentacene-doped tetracene crystals.[72] [d] Value taken from the lowest energy singlet–triplet absorption in single crystals at 4.2 K.[73] [e] Value taken from singlet oxygen sensitization experiments.[74] [f] Value taken from ref. 75. [g] Value taken from triplet energy transfer experiments in ref. 76. [h] Values of E_{aT1} for molecules **1–13** taken from ref. 49.

triphenylene (**1**), coronene (**13**) and benzene (**14**) were lowered in the excited $^3\pi\pi^*$ state. Experimental values of E_{T_1}, shown in Table 1, were mostly taken from phosphorescence measurements. While this was not always possible, the highly localized nature of triplet excitons[69] results in the local environment playing a minimal role in perturbing the value of E_{T_1} (see Table 6.3 in ref. 70 for a list of results using different experimental conditions). For instance, E_{T_1} of tetracene in ethyl iodide and in crystalline form are respectively 1.27 eV[9] and 1.25 eV.[71]

Fig. 2(a) shows the experimental *versus* calculated lowest singlet–triplet energy differences (E_{exp} and E_{calc}, respectively). These plots were fit with a linear equation,

$$E_{calc} = mE_{exp} + y_0, \quad (1)$$

and the values of m and y_0 are given in Table 2. Using the results of the training set, we predict the triplet energy, $E_{pred} = \frac{E_{calc} - y_0}{m}$, of the molecules in the first test set. The mean absolute deviations, $M = \sum |E_{exp} - E_{pred}|/N$ where N is the number of molecules in the test set, are plotted in Fig. 2(b) as a measure of the efficacy of a calculation method. It is clear that the use of DFT to optimize the geometry of these molecules gives excellent correlation between experiment and theory.

Table 2 shows the gradient, m, and the y-intercept, y_0, values. Clearly, the TD-DFT B3LYP/cc-pVTZ study by Parac and Grimme provides the best match between experiment and calculation.[49] The Pearson's r value from the results of Parac and Grimme using B3LYP/cc-pVTZ was 0.9878.[49] In contrast, our results using B3LYP/3-21G give a value of 0.9980. By exploiting the systematic error from the training set and the computationally cheaper option of using a 3-21G basis set we predict singlet–triplet energy gaps closer to the experimental value. However, it should be noted that the work of Parac and Grimme was conducted using the optimized ground state geometry to compare their results with optical absorption experiments. Since the time independent DFT calculations in Fig. 2 are of the adiabatic triplet energy, we should also compare their results with the vertical transition energies presented in Fig. S1 (ESI†).

3.2. Extension to more complex molecules

The B3LYP/3-21G level of theory was chosen for further calculations since an agreeable trade-off between computational expense and accuracy was achieved. The value of E_{T_1} was calculated for the molecules shown in Fig. 3 to investigate whether this method can be utilized to accurately predict the lowest triplet energy of extended π chromophores which contain N or O atoms. The predicted values, E_{pred}, are given in Table S1 (ESI†). For most of the studied molecules the value of $\Delta E = E_{exp} - E_{pred}$ was $\lesssim 0.05$ eV. However, the triplet energies are significantly underestimated for molecules **33–36**.

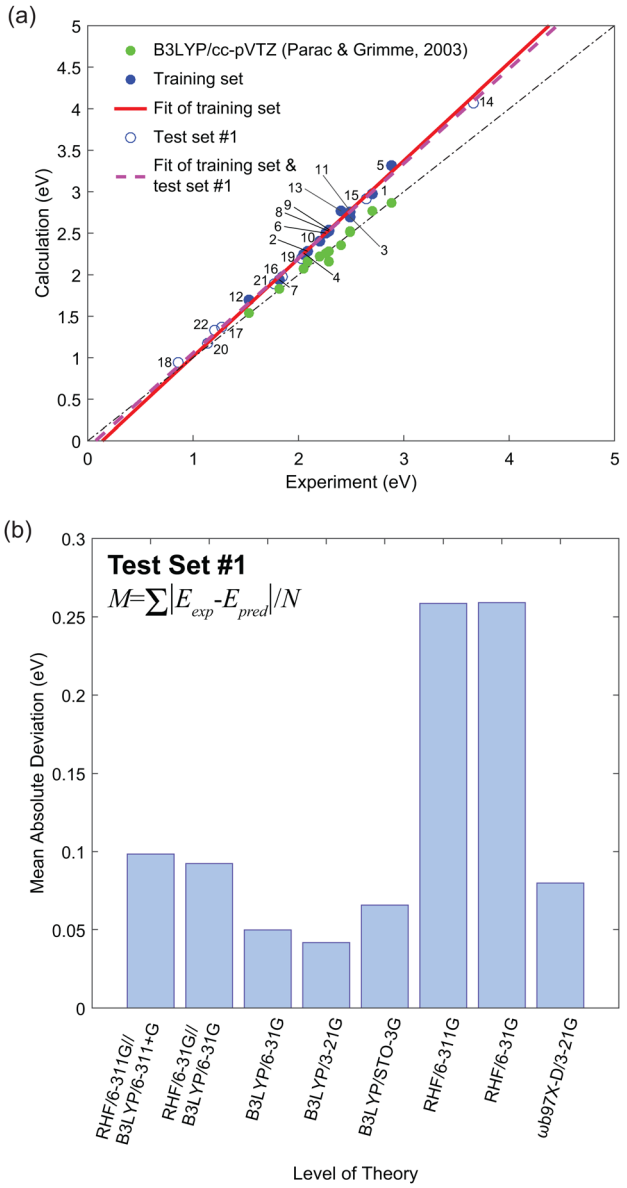

Fig. 2 (a) The B3LYP/3-21G calculated first excited triplet state energy, E_{calc}, as a function of experimental values, E_{exp}. Closed and open circles respectively represent molecules in the training set and test set 1. The red line shows a linear fit of the training set and the dashed pink line is the fit to both the training set and the first test set. The dot-dashed line is $E_{calc} = E_{exp}$. (b) The mean absolute deviation of the predicted values of the first test set using the results of the training set calculations.

Table 2 The fitted values of m and y_0 for different levels of theory using the data in Table 1. The Pearson's r values are also given. Standard errors in the last significant figure are given in parentheses

Level of theory	m	y_0	Pearson's r
Training set			
RHF/6-311G//B3LYP/6-311+G	1.24(3)	−0.28(7)	0.9962
RHF/6-31G//B3LYP/6-31G	1.24(4)	−0.28(9)	0.9947
B3LYP/6-31G	1.19(5)	−0.2(1)	0.9912
B3LYP/3-21G	1.18(4)	−0.2(1)	0.9929
B3LYP/STO-3G	1.22(7)	−0.1(2)	0.9811
HF/6-311G	1.2(3)	−0.1(6)	0.7989
HF/6-31G	1.2(3)	−0.1(6)	0.7958
ωb97x-D/3-21G	1.24(8)	0.0(2)	0.9764
B3LYP/cc-pVTZ[a]	0.99(5)	0.0(1)	0.9884
Training set and first test set			
RHF/6-311G//B3LYP/6-311+G	1.11(2)	−0.00(5)	0.9962
RHF/6-31G//B3LYP/6-31G	1.12(2)	−0.02(5)	0.9962
B3LYP/6-31G	1.14(2)	−0.13(4)	0.9974
B3LYP/3-21G	1.14(2)	−0.09(4)	0.9980
B3LYP/STO-3G	1.17(3)	−0.03(6)	0.9940
HF/6-311G	1.2(1)	−0.2(3)	0.9102
HF/6-31G	1.2(1)	−0.2(3)	0.9104
ωb97x-D/3-21G	1.17(4)	0.08(8)	0.9905
Proposed parameters for future calculations[b]			
B3LYP/3-21G	1.12(1)	−0.04(2)	0.9985

[a] Parameters calculated using values reported in ref. 49 for a vertical transition from the optimized ground state geometry. [b] Values calculated using the results from the training set and both test sets for $^1\pi\pi$–$^3\pi\pi^*$ energy differences in Jahn–Teller inactive systems. We suggest that these parameters be used for future predictive calculations.

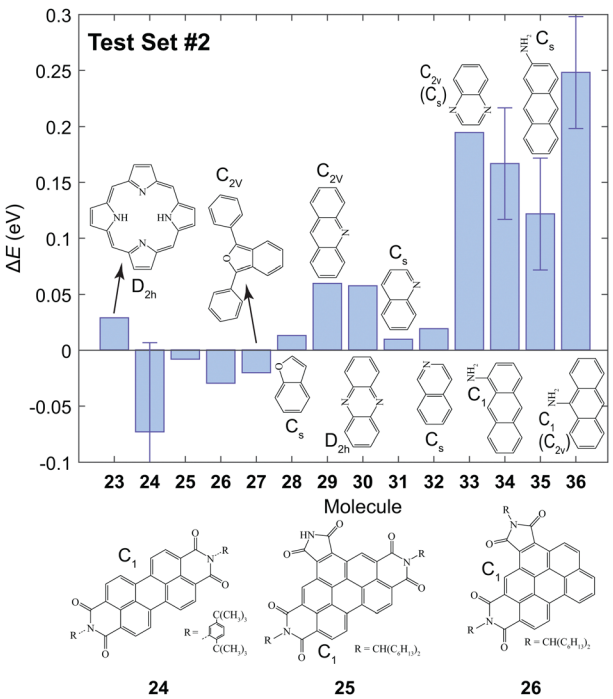

Fig. 3 The values of ΔE for the second test set using the results from the training set and the first test set. The errors arise from the reported experimental uncertainty in ref. 12 and 77 for **24** and the amino-anthracenes (**34–36**), respectively. Experimental values are given in Table S1 (ESI†).

In quinoxaline **33**, the predicted E_{T_1} was underestimated by 0.19 eV. In this molecule, the T_1 and S_1 states are ($\pi\pi^*$) and ($n\pi^*$), respectively.[78] However, the T_1 state was incorrectly calculated to be ($n\pi^*$) using B3LYP/3-21G. This incorrect assignment of the lowest triplet state means that a reasonable prediction cannot be achieved, and is a limitation of the proposed method. One should ensure that the calculated T_1 is $^3\pi\pi^*$ before implementing this method.

Poor predictions were also made for the amino-anthracenes (**34–36**) which contain sp^2 hybridized N atoms. Moreover, experimental reports of the triplet energy of amino-anthracenes are independent of the position of the amine group.

In the calculations there are significant differences between the values of E_{T_1} of **34–36**. Upon examination of the HOMO and LUMO it is clear that the $^1\pi\pi \rightarrow {}^3\pi\pi^*$ transition has significant charge-transfer character since electron density is shifted from the N atom to the π system. Evidently, this is not accounted for using the proposed approach. Attempts to correct for the asymptotic nature of the wavefunction using the hybrid functional ωb97x-D did not yield more accurate results. We conclude that the predictive power using the parameters in Table 2 is limited to systems with where the $^1\pi\pi \rightarrow {}^3\pi\pi^*$ transition does not have considerable charge-transfer character.

3.3. Predictions

In Table 2 we report values of y_0, and gradient, m. Using the data in the final row, we predict the singlet–triplet energy gaps of the molecules shown in Fig. 4. These molecules are of interest for both SF and TTA experiments, however their lowest singlet–triplet energy difference have not been directly experimentally measured.

The triisopropylsilylethynyl moiety has been used to increase the solubility and stability of linear polyacences, as in **37**[79] and **38**.[80] SF has already been reported for both species, which have respective S_1 energies of 2.25 eV[69] and 1.75 eV.[29] As such, we expect the T_1 energies to be less than or approximately equal to 1.13 eV and 0.88 eV, respectively, in accordance with the result in Fig. 4. However, TTA has also been reported in **37**, suggesting that the triplet pair state is approximately degenerate with the S_1 state.[69] As such, we expect the T_1 energy of **37** to be approximately (withing a few kT = 0.026 eV at room temperature) 1.13 eV, and the result shown in Fig. 4 underestimates this by 0.11 eV.

The perylene moiety with attached anhydride or imide groups (molecules **39–42**) has been used in both SF and TTA experiments.[31–33] The predicted triplet energies of the anhydride and imide are similar. Upon examination of the HOMO and LUMO of these species it is clear that this similarity arises because there is very little electron density lying on the sp^2 hybridized N or O atoms. Unfortunately there is little experimental data available to ascertain whether the values of E_{pred} in Fig. 4 are reasonable. A recent report suggested that intramolecular SF in covalently linked perylene monoimide (PMI, **40**) is unlikely to occur because the T_1 energy is greater than half the vibrationally relaxed S_1 energy of 2.29 eV.[81] This accords with the result of E_{pred} = 1.39 eV, however more accurate data of the T_1 energy has not been reported.

$$O_2^*\left(^1\Delta_g\right) + {}^1V_0 \rightarrow O_2\left(^3\Sigma_g^-\right) + {}^3V_1^* \quad (2)$$

$$O_2^*\left(^1\Delta_g\right) + {}^3V_1^* \rightarrow O_2\left(^3\Sigma_g^-\right) + {}^1V_1^* \quad (3)$$

$$^1V_1^* \rightarrow {}^1V_0 + h\nu \quad (4)$$

Singlet oxygen ($O_2(^1\Delta_g)$) may have an energy slightly less that of violanthrone's triplet and eqn (2) would still proceed. Indeed, similar experiments were successfully carried out with rubrene, where some 0.35 eV is required for the reaction to proceed.[82] Moreover, a violanthrone derivative has been shown to undergo TTA.[83] Combining these results, violanthrone's triplet state energy is (i) similar to (within a few kT) or less than that of singlet oxygen (*ca.* 0.98 eV); (ii) similar to or greater than the difference in energy of the S_1 (1.97 eV) state and singlet oxygen, *i.e.* $\gtrsim$0.99 eV; and (iii) greater than half the energy of the S_1 state, *i.e.* >0.99 eV. Under these constraints, one expects the triplet energy to be *ca.* 1 eV, which accords with the result in Fig. 4.

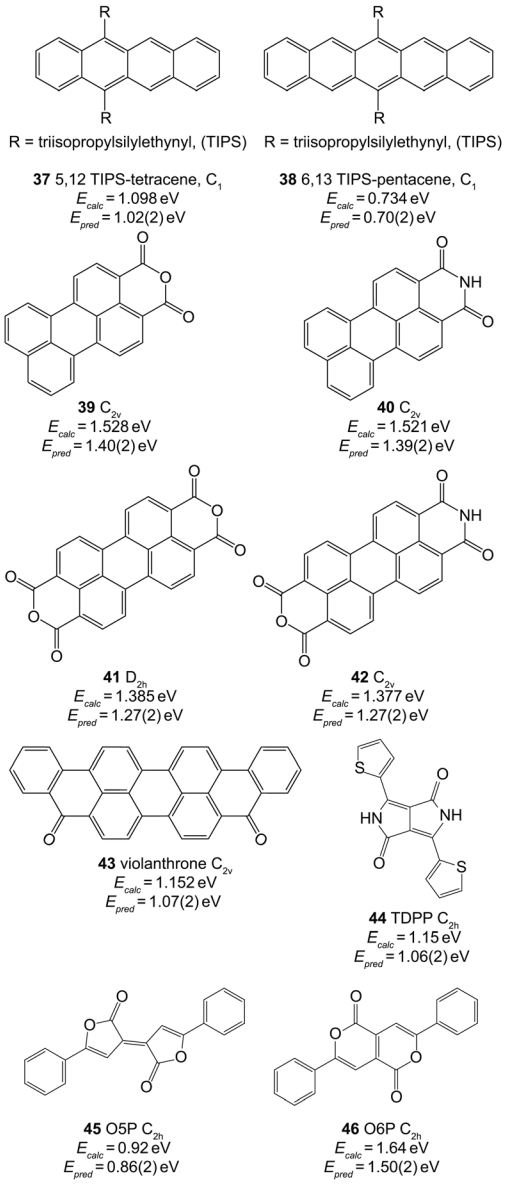

Fig. 4 Extended π systems and predicted values of E_{T_1} using B3LYP/3-21G and the parameters in the final row of Table 2. The symmetries used for the calculations are given next to each molecule.

Diketopyrrolopyrroles (DPP) are another class of materials which are promising for SF.[84] Karsten *et al.* measured the triplet energy of a thienyl derivative of DPP to be 1.1 eV.[85] This material only differed from **44** by an alkyl chain replacing the hydrogen at the pyrrole nitrogens. As we can see from Fig. 4, this agrees extremely well with our prediction of 1.06 eV.

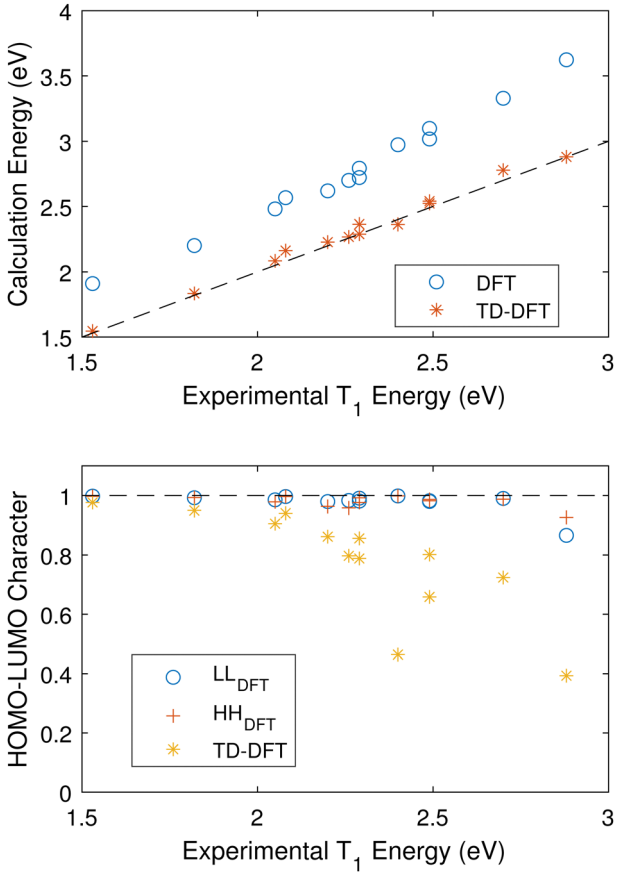

Fig. 5 (a) Calculated vertical triplet energies as a function experimental values. Both DFT and TD-DFT were carried out at the optimized S_0 geometry using B3LYP/cc-pVTZ. The DFT systematically overestimates the value of the triplet. (b) The HOMO–LUMO character of the S_0 to T_0 transition as output by TD-DFT and estimated using eqn (5) for DFT.

Finally, Pechmann dyes have very recently been shown to undergo SF for the five-membered-ring isomer (**45**, O5P), but not for the six-membered ring isomer (**46** O6P).[86] While no experimental measurements of the T_1 energy exist, our predictions accord with this recent work (where we have removed a methyl group as compared to the work in ref. 86). The thin-film singlet energy of O5P and O6P are approximately 2.2 eV and 2.6 eV, respectively (Fig. S17 of ref. 86). As such, our predicted triplet energies of 0.86 eV and 1.50 eV would allow for SF to occur in the former, but not the latter.

3.4. Why does this work?

We are left with an efficient and accurate way of calculating the T_1 energy of a wide class of molecules. We are subtracting the energy of the geometry optimized S_0 state from the geometry optimized T_1 state; this yields a systematic error that increases with the energy of T_1. The question remains: why does this work?

The gradients and offsets listed in Table 2 do not display any significant trend with increasing the basis set level of theory. Further, the results of B3LYP are very similar to ωb97x-D, suggesting that the chosen functional has a limited effect.

However, the TD-DFT calculations of Parac and Grimme (B3LYP) were rather accurate (see Fig. 2) before applying any post-calculation empirical correction.[49] This suggests that the systematic error observed in our DFT calculations are corrected for by TD-DFT.

As such, we attempt to compare the vertical transition energies from an optimized S_0 ground state using both DFT and TD-DFT and a B3LYP/cc-pVTZ level of theory. Fig. 5(a) shows that TD-DFT calculates excited triplet energies which are in good agreement with the experimental values for the training set.

Fig. 5(b) compares the S_0 HOMO–LUMO character of the S_0 to T_1 transitions using TD-DFT and DFT. For TD-DFT this is simply generated in the calculation output. For DFT, we estimate this value by calculating the overlap of the LUMOs calculated for S_0 and T_1,

$$\mathrm{LL_{DFT}} = |\langle \chi_{\mathrm{L,S_0}} | \mathbf{S} | \chi_{\mathrm{L,T_1}} \rangle|^2, \quad (5)$$

where $\chi_{\mathrm{L,S_0/T_1}}$ are the molecular orbitals of the LUMOs of the S_0 and T_1 states. The 1-electron basis function overlap matrix **S** is used to account for the non-orthogonal 1-election basis. Since the analogous HOMO–HOMO overlap $\mathrm{HH_{DFT}}$ is close to $\mathrm{LL_{DFT}}$ for all triplet energies (see Fig. 5(b)), we use $\mathrm{LL_{DFT}}$ a proxy for the amount of HOMO–LUMO character captured in DFT. Upon examination of Fig. 5(b) we note that as E_{T_1} increases the HOMO–LUMO character of the transition decreases for both DFT and TD-DFT; however this effect is far greater in TD-DFT. We suggest that the systematic error arises because time independent DFT is constrained to overestimate the HOMO–LUMO character of S_0 to T_1 transition. Fortuitously, it appears that this error is linear over the range of triplet energies that are relevant to most technological applications.

4. Conclusions

Using the data in the final row of Table 2 one can use B3LYP/3-21G to easily and accurately predict the singlet–triplet ($^1\pi\pi$–$^3\pi\pi^*$) energy difference in neutral extended π chromophores. However, when either the ground singlet, first excited singlet, or ground triplet states have significant non-bonding or charge-transfer character the simple empirical model presented here is not sufficient. While this work will not replace sophisticated computations of E_{T_1}, it provides the experimental chemist with a inexpensive calculation for this difficult to measure quantity. We propose that this method may be used to rapidly screen for new singlet fission and TTA candidates. A step-by-step method is provided in the ESI.†

Data availability

The code for DFT can be found at **https://www.msg.chem.iastate.edu/gamess/index.html** with **https://aip.scitation.org/doi/10.1063/5.0005188**. The versions of the code employed for this study are outlined in the Methodology section.

Conflicts of interest

There are no conflicts of interest to declare.

Acknowledgements

MJYT acknowledges receipt of an Australian Research Council Future Fellowship (FT230100002). This work was supported by the Australian Research Council (Centre of Excellence in Exciton Science CE170100026). MJYT and KLKL acknowledge use of computing resources from the NeCTAR Research Cloud **https://www.nectar.org.au**. NeCTAR is an Australian Government project conducted as part of the Super Science initiative and financed by the Education Investment Fund and the National Collaborative Research Infrastructure Strategy (NCRIS). This research includes computations using the computational cluster Katana supported by Research Technology Services at UNSW Sydney. This program has been supported by the Australian Government through the Australian Renewable Energy Agency (ARENA). Responsibility for the views, information or advice expressed herein is not accepted by the Australian Government.

Notes and references

1 M. B. Smith and J. Michl, *Chem. Rev.*, 2010, **110**, 6891–6936.
2 M. B. Smith and J. Michl, *Annu. Rev. Phys. Chem.*, 2013, **64**, 361–386.
3 T. F. Schulze and T. W. Schmidt, *Energy Environ. Sci.*, 2015, **8**, 103–125.
4 M. J. Y. Tayebjee, D. R. McCamey and T. W. Schmidt, *J. Phys. Chem. Lett.*, 2015, **6**, 2367–2378.
5 A. J. Baldacchino, M. I. Collins, M. P. Nielsen, T. W. Schmidt, D. R. McCamey and M. J. Y. Tayebjee, *Chem. Phys. Rev.*, 2022, **3**, 21304.
6 S. N. Sanders, T. H. Schloemer, M. K. Gangishetty, D. Anderson, M. Seitz, A. O. Gallegos, R. C. Stokes and D. N. Congreve, *Nature*, 2022, **604**, 474–478.
7 R. M. Jacobberger, Y. Qiu, M. L. Williams, M. D. Krzyaniak and M. R. Wasielewski, *J. Am. Chem. Soc.*, 2022, **144**, 2276–2283.
8 R. J. Hudson, T. S. C. MacDonald, J. H. Cole, T. W. Schmidt, T. A. Smith and D. R. McCamey, *Nat. Rev. Chem.*, 2024, **8**, 136–151.
9 S. P. Mcglynn, M. Kasha and T. Azumi, *J. Chem. Phys.*, 1964, **40**, 507–515.
10 I. J. Grahambryce and J. M. Corkill, *Nature*, 1960, **186**, 965–966.
11 S. Reineke and M. A. Baldo, *Sci. Rep.*, 2014, **4**, 3797.
12 W. E. Ford and P. V. Kamat, *J. Phys. Chem.*, 1987, **91**, 6373–6380.
13 P. M. Zimmerman, F. Bell, D. Casanova and M. Head-Gordon, *J. Am. Chem. Soc.*, 2011, **133**, 19944–19952.
14 J. J. Burdett, A. M. Muller, D. Gosztola and C. J. Bardeen, *J. Chem. Phys.*, 2010, **133**, 144506.
15 J. J. Burdett, D. Gosztola and C. J. Bardeen, *J. Chem. Phys.*, 2011, **135**, 214508.
16 J. J. Burdett and C. J. Bardeen, *J. Am. Chem. Soc.*, 2012, **134**, 8597–8607.
17 J. J. Burdett, G. B. Piland and C. J. Bardeen, *Chem. Phys. Lett.*, 2013, **585**, 1–10.
18 J. J. Burdett and C. J. Bardeen, *Acc. Chem. Res.*, 2013, **46**, 1312–1320.
19 P. J. Jadhav, A. Mohanty, J. Sussman, J. Lee and M. A. Baldo, *Nano Lett.*, 2011, **11**, 1495–1498.
20 D. N. Congreve, J. Lee, N. J. Thompson, E. Hontz, S. R. Yost, P. D. Reusswig, M. E. Bahlke, S. Reineke, T. Van Voorhis and M. A. Baldo, *Science*, 2013, **340**, 334–337.
21 W. L. Chan, M. Ligges and X. Y. Zhu, *Nat. Chem.*, 2012, **4**, 840–845.
22 S. T. Roberts, R. E. McAnally, J. N. Mastron, D. H. Webber, M. T. Whited, R. L. Brutchey, M. E. Thompson and S. E. Bradforth, *J. Am. Chem. Soc.*, 2012, **134**, 6388–6400.
23 J. N. Mastron, S. T. Roberts, R. E. McAnally, M. E. Thompson and S. E. Bradforth, *J. Phys. Chem. B*, 2013, **117**(49), 15519–15526.
24 M. J. Y. Tayebjee, R. G. C. R. Clady and T. W. Schmidt, *Phys. Chem. Chem. Phys.*, 2013, **15**, 14797–14805.
25 M. W. B. Wilson, A. Rao, K. Johnson, S. Gélinas, R. di Pietro, J. Clark and R. H. Friend, *J. Am. Chem. Soc.*, 2013, **135**, 16680–16688.
26 G. B. Piland and C. J. Bardeen, *J. Phys. Chem. Lett.*, 2015, **6**, 1841–1846.
27 W. L. Chan, M. Ligges, A. Jailaubekov, L. Kaake, L. Miaja-Avila and X. Y. Zhu, *Science*, 2011, **334**, 1541–1545.
28 B. Ehrler, B. J. Walker, M. L. Böhm, M. W. B. Wilson, Y. Vaynzof, R. H. Friend and N. C. Greenham, *Nat. Commun.*, 2012, **3**, 1019.
29 B. J. Walker, A. J. Musser, D. Beljonne and R. H. Friend, *Nat. Chem.*, 2013, **5**, 1019–1024.
30 A. J. Musser, M. Liebel, C. Schnedermann, T. Wende, T. B. Kehoe, A. Rao and P. Kukura, *Nat. Phys.*, 2015, **11**, 352–357.
31 C. Ramanan, A. L. Smeigh, J. E. Anthony, T. J. Marks and M. R. Wasielewski, *J. Am. Chem. Soc.*, 2011, **134**, 386–397.
32 K. M. Lefler, K. E. Brown, W. A. Salamant, S. M. Dyar, K. E. Knowles and M. R. Wasielewski, *J. Phys. Chem. A*, 2013, **117**, 10333–10345.
33 S. W. Eaton, L. E. Shoer, S. D. Karlen, S. M. Dyar, E. A. Margulies, B. S. Veldkamp, C. Ramanan, D. A. Hartzler, S. Savikhin, T. J. Marks and M. R. Wasielewski, *J. Am. Chem. Soc.*, 2013, **135**, 14701–14712.
34 J. C. Johnson, A. J. Nozik and J. Michl, *J. Am. Chem. Soc.*, 2010, **132**, 16302–16303.
35 X. Feng, A. B. Kolomeisky and A. I. Krylov, *J. Phys. Chem. C*, 2014, **118**, 19608–19617.
36 C. C. Gradinaru, J. T. M. Kennis, E. Papagiannakis, I. H. M. van Stokkum, R. J. Cogdell, G. R. Fleming, R. A. Niederman and R. van Grondelle, *Proc. Natl. Acad. Sci. U. S. A.*, 2001, **98**, 2364–2369.
37 C. Wang and M. J. Tauber, *J. Am. Chem. Soc.*, 2010, **132**, 13988–13991.
38 C. Wang, D. E. Schlamadinger, V. Desai and M. J. Tauber, *ChemPhysChem*, 2011, **12**, 2891–2894.

39 C. Wang, C. J. Berg, C. C. Hsu, B. A. Merrill and M. J. Tauber, *J. Phys. Chem. B*, 2012, **116**, 10617–10630.
40 A. J. Musser, M. Maiuri, D. Brida, G. Cerullo, R. H. Friend and J. Clark, *J. Am. Chem. Soc.*, 2015, **137**, 5130–5139.
41 S. Baluschev, T. Miteva, V. Yakutkin, G. Nelles, A. Yasuda and G. Wegner, *Phys. Rev. Lett.*, 2006, **97**, 143903.
42 T. N. Singh-Rachford and F. N. Castellano, *Coord. Chem. Rev.*, 2010, **254**, 2560–2573.
43 T. W. Schmidt and F. N. Castellano, *J. Phys. Chem. Lett.*, 2014, **5**, 4062–4072.
44 D. Jacquemin, V. Wathelet, E. A. Perpète and C. Adamo, *J. Chem. Theory Comput.*, 2009, **5**, 2420–2435.
45 M. J. G. Peach and D. J. Tozer, *J. Phys. Chem. A*, 2012, **116**, 9783–9789.
46 A. F. Morrison, Z.-Q. You and J. M. Herbert, *J. Chem. Theory Comput.*, 2014, **10**, 5366–5376.
47 D. Jacquemin, E. A. Perpète, I. Ciofini and C. Adamo, *J. Chem. Theory Comput.*, 2010, **6**, 1532–1537.
48 M. J. G. Peach, M. J. Williamson and D. J. Tozer, *J. Chem. Theory Comput.*, 2011, **7**, 3578–3585.
49 M. Parac and S. Grimme, *Chem. Phys.*, 2003, **292**, 11–21.
50 J. P. Merrick, D. Moran and L. Radom, *J. Phys. Chem. A*, 2007, **111**, 11683–11700.
51 M. W. Schmidt, K. K. Baldridge, J. A. Boatz, S. T. Elbert, M. S. Gordon, J. H. Jensen, S. Koseki, N. Matsunaga, K. A. Nguyen, S. Su, T. L. Windus, M. Dupuis and J. A. Montgomery, *J. Comput. Chem.*, 1993, **14**, 1347–1363.
52 M. S. Gordon and M. W. Schmidt, in *Chapter 41 - Advances in electronic structure theory: GAMESS a decade later*, ed. C. E. Dykstra, G. Frenking, K. S. Kim and G. E. Scuseria, Elsevier, Amsterdam, 2005, pp. 1167–1189.
53 C. C. J. Roothaan, *Rev. Mod. Phys.*, 1951, **23**, 69–89.
54 A. D. Becke, *J. Chem. Phys.*, 1993, **98**, 5648–5652.
55 P. J. Stephens, F. J. Devlin, C. F. Chabalowski and M. J. Frisch, *J. Phys. Chem.*, 1994, **98**, 11623–11627.
56 R. H. Hertwig and W. Koch, *Chem. Phys. Lett.*, 1997, **268**, 345–351.
57 J.-D. Chai and M. Head-Gordon, *J. Chem. Phys.*, 2008, **128**, 084106.
58 J.-D. Chai and M. Head-Gordon, *Phys. Chem. Chem. Phys.*, 2008, **10**, 6615–6620.
59 W. J. Hehre, R. F. Stewart and J. A. Pople, *J. Chem. Phys.*, 1969, **51**, 2657–2664.
60 W. J. Hehre, R. Ditchfield, R. F. Stewart and J. A. Pople, *J. Chem. Phys.*, 1970, **52**, 2769–2773.
61 J. S. Binkley, J. A. Pople and W. J. Hehre, *J. Am. Chem. Soc.*, 1980, **102**, 939–947.
62 M. S. Gordon, J. S. Binkley, J. A. Pople, W. J. Pietro and W. J. Hehre, *J. Am. Chem. Soc.*, 1982, **104**, 2797–2803.
63 R. Ditchfield, W. J. Hehre and J. A. Pople, *J. Chem. Phys.*, 1971, **54**, 724–728.
64 W. J. Hehre, R. Ditchfield and J. A. Pople, *J. Chem. Phys.*, 1972, **56**, 2257–2261.
65 R. Krishnan, J. S. Binkley, R. Seeger and J. A. Pople, *J. Chem. Phys.*, 1980, **72**, 650–654.
66 T. Clark, J. Chandrasekhar, G. W. Spitznagel and P. V. R. Schleyer, *J. Comput. Chem.*, 1983, **4**, 294–301.
67 G. M. J. Barca, C. Bertoni, L. Carrington, D. Datta, N. D. Silva, J. E. Deustua, D. G. Fedorov, J. R. Gour, A. O. Gunina, E. Guidez, T. Harville, S. Irle, J. Ivanic, K. Kowalski, S. S. Leang, H. Li, W. Li, J. J. Lutz, I. Magoulas, J. Mato, V. Mironov, H. Nakata, B. Q. Pham, P. Piecuch, D. Poole, S. R. Pruitt, A. P. Rendell, L. B. Roskop, K. Ruedenberg, T. Sattasathuchana, M. W. Schmidt, J. Shen, L. Slipchenko, M. Sosonkina, V. Sundriyal, A. Tiwari, J. L. G. Vallejo, B. Westheimer, M. Włoch, P. Xu, F. Zahariev and M. S. Gordon, *J. Chem. Phys.*, 2020, **152**, 154102.
68 T. H. Dunning, *J. Chem. Phys.*, 1989, **90**, 1007–1023.
69 S. L. Bayliss, A. D. Chepelianskii, A. Sepe, B. J. Walker, B. Ehrler, M. J. Bruzek, J. E. Anthony and N. C. Greenham, *Phys. Rev. Lett.*, 2014, **112**, 238701.
70 J. B. Birks, *Photophysics of Aromatic Molecules*, John Wiley & Sons, London, 1970.
71 Y. Tomkiewicz, R. P. Groff and P. Avakian, *J. Chem. Phys.*, 1971, **54**, 4504–4507.
72 J. Burgos, M. Pope, C. E. Swenberg and R. R. Alfano, *Phys. Status Solidi B*, 1977, **83**, 249–256.
73 R. H. Clarke and R. M. Hochstrasser, *J. Mol. Spectrosc.*, 1969, **32**, 309–319.
74 W. G. Herkstroeter and P. B. Merkel, *J. Photochem.*, 1981, **16**, 331–341.
75 T. N. Singh-Rachford, J. Lott, C. Weder and F. N. Castellano, *J. Am. Chem. Soc.*, 2009, **131**, 12007–12014.
76 C. Burgdorff, T. Kircher and H. G. Lohmannsroben, *Spectrochim. Acta, Part A*, 1988, **44**, 1137–1141.
77 K. Rotkiewicz and Z. R. Grabowski, *Trans. Faraday Soc.*, 1969, **65**, 3263–3278.
78 S. G. Hadley, *J. Phys. Chem.*, 1971, **75**, 2083–2086.
79 S. A. Odom, S. R. Parkin and J. E. Anthony, *Org. Lett.*, 2003, **5**, 4245–4248.
80 J. E. Anthony, J. S. Brooks, D. L. Eaton and S. R. Parkin, *J. Am. Chem. Soc.*, 2001, **123**, 9482–9483.
81 R. J. Lindquist, K. M. Lefler, K. E. Brown, S. M. Dyar, E. A. Margulies, R. M. Young and M. R. Wasielewski, *J. Am. Chem. Soc.*, 2014, **136**, 14912–14923.
82 T. Wilson, *J. Am. Chem. Soc.*, 1969, **91**, 2387–2388.
83 E. M. Gholizadeh, S. K. K. Prasad, L. V. Gillan, M. P. Nielsen, N. J. Ekins-Daukes, D. R. McCamey, M. J. Y. Tayebjee and T. W. Schmidt, *J. Phys. Chem. C*, 2021, **125**, 22464–22471.
84 P. E. Hartnett, E. A. Margulies, C. M. Mauck, S. A. Miller, Y. Wu, Y.-L. Wu, T. J. Marks and M. R. Wasielewski, *J. Phys. Chem. B*, 2016, **120**, 1357–1366.
85 B. P. Karsten, R. K. M. Bouwer, J. C. Hummelen, R. M. Williams and R. A. J. Janssen, *Photochem. Photobiol. Sci.*, 2010, **9**, 1055–1065.
86 A. V. Girija, W. Zeng, W. K. Myers, R. C. Kilbride, D. T. W. Toolan, C. Zhong, F. Plasser, A. Rao and H. Bronstein, *J. Am. Chem. Soc.*, 2024, **146**, 18253–18261.